Simple and Accurate Assessment of Forward Cardiac Output by Use of 1-^{11}C-Acetate PET Verified in a Pig Model

Jens Sörensen, MD[1,2]; Elisabeth Ståhle, MD, PhD[3]; Bengt Långström, PhD[2]; Gunnar Frostfeldt, MD, PhD[4]; Gerhard Wikström, MD, PhD[4]; and Göran Hedenstierna, MD, PhD[1]

[1]Clinical Physiology, Department of Medical Sciences, Academic Hospital, Uppsala, Sweden; [2]Uppsala University PET Centre, Uppsala, Sweden; [3]Thoracic Surgery, Department of Medical Sciences, Academic Hospital, Uppsala, Sweden; and [4]Cardiology, Department of Medical Sciences, Academic Hospital, Uppsala, Sweden

Dynamic 1-^{11}C-acetate PET (AC-PET) allows quantification of myocardial blood flow and oxidative metabolism. We wanted to determine the accuracy of AC-PET in measuring cardiac output (CO) using first-pass analysis and the indicator dilution principle. Further, we wanted to investigate the pulmonary uptake of acetate in relation to left atrial filling pressures and ventricular function. **Methods:** Twenty-four steady-state experiments were performed in 5 domestic pigs. Pulmonary capillary wedge pressure (PCWP) and CO by thermodilution (CO_{thermo}) were recorded invasively simultaneous with AC-PET scans at baseline ($n = 9$), dobutamine infusion ($n = 6$), high-dose metoprolol and morphine ($n = 6$), and angiotensinamide infusion ($n = 3$). 1-^{11}C-Acetate was injected as a rapid manual bolus. Regions of interest (ROIs) were placed in the right (RV) and left (LV) heart cavities. Time–activity curves were constructed and the area under the curve (AUC) was integrated from beginning the scan to the time of visually determined recirculation by simple arithmetic. CO by PET (CO_{PET}) was calculated as injected dose/AUC. Image handling and curve analysis were repeated by a blinded observer. Total pulmonary extravascular retention of ^{11}C, expressed as percentage of injected dose (lung-uptake %ID), was measured using a combination of transmission, ^{15}O-carbon monoxide, and AC-PET scans. **Results:** CO_{thermo} ranged from 2.1 to 8.2 L/min. CO_{PET} determined from both LV and RV was linearly related to CO_{thermo} with slopes close to 1 (LV, $r = 0.98$; RV, $r = 0.96$; both $P < 0.001$). Interobserver reproducibility was $r = 0.98$, $P < 0.001$. The PCWP range was 6–14 mm Hg and the lung-uptake %ID was 2.7–8.5 %ID. When normalized to baseline, lung-uptake %ID was correlated with PCWP ($r = 0.56$, $P = 0.01$) and linearly correlated with LV input resistance (PCWP divided by CO_{thermo}; $r = 0.91$, $P < 0.001$). When both lung-uptake %ID and stroke volume were normalized to baseline, a piecewise linear relation was found ($r = 0.95$, $P < 0.001$). **Conclusion:** Our results suggest that measurements of CO by AC-PET are feasible and accurate. Using RV ROIs might favor CO measurements by any injectable PET tracer. The lung-uptake %ID might be useful in evaluation of pulmonary congestion, but further studies are needed.

Key Words: cardiac output; acetate; PET; tracer kinetics

J Nucl Med 2003; 44:1176–1183

Since the early 1980s, PET with 1-^{11}C-acetate as a tracer (AC-PET) has been used for the noninvasive assessment of myocardial oxidative metabolism. The concept has been validated in animal and human studies as well as in several clinical investigations. The early clearance rate of ^{11}C from the myocardium correlates significantly and linearly with invasively measured myocardial oxygen consumption over a wide range of physiologic and pathologic conditions (*1*). Because 1-^{11}C-acetate has a relatively high first-pass extraction in myocardial tissue it has been advocated also as a marker of myocardial perfusion. Quantification of resting and hyperemic blood flows are possible and have been tested against previously established techniques with good results (*2*). Further, estimates of oxygen consumption with AC-PET have been used to determine myocardial efficiency in healthy volunteers and various disease states by incorporating MRI- or equilibrium radionuclide angiography-derived stroke volume (SV) measurements and AC-PET data into a single work-metabolic index (WMI) (*3*). This method is indeed intuitively appealing but has a drawback in that it needs additional scans to measure SV. Instead, the direct determination of cardiac output (CO), and hence SV, might be accomplished simultaneously during an AC-PET scan by first-pass analysis and the indicator-dilution method.

The main purpose of this study was to compare the accuracy of AC-PET–derived CO with validated invasive measurements of CO in an animal model. As a second aim, we wanted to measure the lung uptake of acetate to see if pulmonary retention affected the accuracy of the CO measurements and also to investigate the relation between the magnitude of lung uptake and cardiac function.

Received Sep. 5, 2002; revision accepted Feb. 13, 2003.

For correspondence or reprints contact: Jens Sörensen, MD, Department of Clinical Physiology and Nuclear Medicine, University Hospital, S-751 85 Uppsala, Sweden.

E-mail: jens.sorensen@pet.uu.se

MATERIALS AND METHODS

Animal Preparation

Five domestic pigs with a weight of 30.8 ± 2.9 kg (mean ± SD) were used. After premedication with tiletamine (6 mg/kg), xylazin (2.2 mg/kg), and morphine (20 mg), the pigs were tracheotomized and ventilated using 40% oxygen gas in nitrogen. Anesthesia was maintained by infusion of morphine (120 mg), ketaminol (5 g), and pancuronium bromide (60 mg) mixed in 1,000 mL Ringer-acetate at a rate of 4 mL/kg/h. Cannulations were performed in carotid arteries and jugular veins. Principles of laboratory animal care were followed and the local animal ethics committee approved the study.

Study Protocol

First, a baseline study was performed once ($n = 5$) or twice ($n = 4$). Then, the CO was elevated by infusing 15–25 μmol/min/kg of dobutamine and measurements were performed when steady state was reached ($n = 6$). After that, 10–15 mg of metoprolol and 10–15 mg of morphine were injected to reduce cardiac contractility and peripheral oxygen needs, thereby lowering CO ($n = 6$). Finally, we infused angiotensinamide (Apoteksbolaget AB) at a rate of 2.5 mg/kg/min to increase the global vascular resistance ($n = 3$). After the last measurements, the pigs were killed by a large intravenous dose of KCl.

Invasive Measurements

CO by thermodilution (CO_{thermo}) was measured by the standard technique (*4*) within 5 min of the corresponding PET scan. Heart rate (HR) as well as pressures in the pulmonary artery (PA) and carotid artery (CA) were monitored throughout the study and recorded immediately before a PET scan sequence. Mean pulmonary capillary wedge pressure (PCWP) was measured just after the CO determination.

SV (mL) was calculated as SV = CO × 1,000/HR. To overcome interindividual differences in heart sizes, SV was also evaluated in relation to PET data after normalization to the baseline investigation in each pig (SV_{norm}). The rate–pressure product (RPP) was calculated as RPP = HR (min) × peak systolic arterial pressure (mm Hg).

Pulmonary arterial vascular resistance (RVascPulm) was calculated as (mean PA pressure [PCWP]) divided by CO_{thermo}. Left ventricular (LV) input resistance was calculated as PCWP divided by CO (mm Hg/[L/min]).

PET Method

A standard clinical Siemens CTI HR+ PET scanner was used, the specifications of which has been described in detail elsewhere (*5*). The scanner was operated in 2-dimensional frame mode. Pigs were placed in the scanner and positioned with the heart and all of the lungs within the field of view after a short scout transmission scan. To reduce the effect of possible changes in pulmonary content of air and blood on lung uptake measurements, a 10-min transmission scan using rotating ^{68}Ge rods was performed before tracer injection for subsequent attenuation correction of emission scans both at baseline and at least once during steady state in pharmacologic perturbations.

To measure pulmonary blood volume, ^{15}O-carbon monoxide (^{15}O-CXO) mixed with air was added to the inhalation gases with a flow of 1.5 L/min at baseline and during stress in each of 3 pigs. ^{15}O-CXO delivery continued for 120 s or until the total counting rate reached 10^5 counts/s. After allowing another 60 s for equilibration, an emission scan was started with one 360-s frame.

1-^{11}C-Acetate (dose range, 58–553 MBq) diluted in 3–4 mL saline was injected simultaneous to scan start. A frame sequence of 12 × 5 s, 6 × 10 s, and 1 × 120 s, comprising 4 min, was used. The injection of 1-^{11}C-acetate was performed as a rapid manual bolus in <2 s, immediately followed by a 10-mL saline manual flush. In 14 experiments, activity was injected directly into the central venous catheter (animals 1, 2, and 4). In the remaining 10 experiments, a peripheral ear vein was used (animals 3 and 5). When the peripheral route was used, we introduced a 3- to 5-s wait between tracer injection and saline flush to study the effect of bolus irregularities on CO measurements.

All emission scans were corrected for attenuation, scatter, and decay and reconstructed to a 128 × 128 matrix with a zoom factor of 2.5, resulting in a pixel size of 2 mm. A Hann filter of 4.2 mm was used, resulting in an in-plane axial full width at half maximum of approximately 6 mm. All emission scans were reconstructed by filtered backprojection.

Regions of interest (ROIs) were defined interactively using the ECAT 7.2.1 software provided by the scanner manufacturer.

Total average lung volume was measured by ROI analysis on transaxial slices of attenuation images. The lungs were delineated from the surrounding solid tissues by a 50% cutoff, thereby leaving out the hilar regions and major central vessels. Lung ROIs were copied to emission scans.

Total lung blood volume (in mL) was calculated from ^{15}O-CXO scans by dividing the total lung ^{15}O activity in becquerels (Bq) by the activity in whole blood (Bq/mL), derived from an ROI within the LV cavity. Fractional lung blood volume was calculated as total lung blood volume divided by total lung volume.

Myocardial ROIs were defined on the final frame of the AC-PET scan from 2 to 4 min after injection. This image was resliced to the short-axis view. Circular ROIs with areas of 1–2 cm^2 were placed centrally in the basal planes of both the right ventricular (RV) and LV cavities. To improve count statistics, 3 or 4 ROIs in consecutive image planes of the LV and 2 ROIs in the RV were linked. An annular ROI with a radial width of 10 mm was positioned circumferentially over the myocardial wall in a midventricular slice of the LV in the short-axis view.

ROI-Based Calculations

Time–activity curves were constructed for all ROIs defined on 1-^{11}C-acetate scans and exported to a personal computer running Windows Excel 2000 for further calculations.

Total activity of ^{11}C in the lungs was measured from 2 to 4 min after injection. Lung ROIs were taken from the most recent transmission scan. Correction for blood-pool spillover was done by subtracting the product of total lung blood volume and ^{11}C concentration in RV from the total lung ^{11}C activity. In the 18 experiments, where directly measured blood-pool volumes were not available, the mean value derived from the 6 ^{15}O-CXO scans was used as a substitute. The total extravascular activity of ^{11}C in the lungs in percentage of the injected dose was used as an index of fractional lung retention (lung-uptake %ID).

The net extraction rate of ^{11}C into myocardial tissue was measured to assess the error in CO by PET (CO_{PET}) induced by myocardial tissue spillover into the cavity ROIs. Activity in the myocardial ROI from 60 to 120 s after injection was divided by the arterial input function from 0 to 120 s, yielding the net extraction rate (in mL/min/mL). Because measurements of true myocardial blood flow (MBF) were not an endpoint, no corrections for blood-pool spillover, limited recovery, or partial tissue extraction were

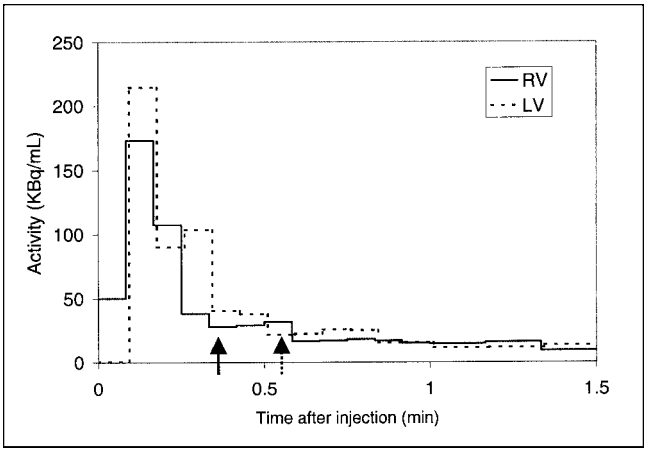

FIGURE 1. Representative time–activity curves recorded from ROI in RV and LV cavities, respectively. Time frame where first pass of bolus ends and recirculation arrives is determined interactively by locating time frame with lowest concentration shortly after injection (arrows). In this case, 244 MBq 1-^{11}C-acetate were injected as rapid bolus directly into superior vena cava during intravenous infusion of 25 μg/kg/min of dobutamine in pig. Irregular activity in LV is seen initially, probably due to variable flow velocity caused by respiration. Division of amount of injected activity by average concentration in cavity during first-pass transit reveals number of milliliters it takes to move entire dose through cavity, which equals CO. Estimates of CO by PET were 6.2 and 5.8 L/min for RV and LV, respectively. CO simultaneously estimated by standard thermodilution technique was 5.8 L/min.

performed. Because functional myocardium increases blood flow in proportion to workload, we tested the derived net extraction rate against RPP to ensure a good surrogate relation toward MBF.

The rationale for calculating CO after a bolus injection relies on the Stewart–Hamilton formula:

$$CO = \frac{I}{\int C(a)dt}, \qquad \text{Eq. 1}$$

where I is injected dose and the denominator is the area under the curve (AUC) of the blood activity plotted against time during the first pass, corrected for recirculation (AUC_{fp}). We integrated AUC_{fp} of both RV and LV time–activity curves by simply summing the time–activity boxes as described in Figure 1. Separating the tail of first-pass activity from recirculation was done interactively on time–activity curve plots. The frame with the lowest activity after the initial first-pass down slope was used as a delimiter. If this notch in the curve was obviously caused by bolus fractionating—that is, the curve had 2 initial peaks—the next local minimum in the curve was chosen.

All ROI analyses and calculations were performed by 1 investigator. A second observer, unaware of all other data, repeated reslicing of cardiac images, RV and LV cavity ROI definition, and first-pass analysis.

Statistical Analysis

Statistical evaluations were done on a personal computer running Windows 2000 and the Statistica 6.0 software package (Statsoft Inc.). Values are expressed as mean ± SD, if not otherwise stated. Nonparametric Spearman rank tests were used for correlative calculations. If linearity could be established, simple linear regression analysis was applied. In 1 case, a relation was obviously nonlinear and piecewise linear regression analysis was applied. CO measurements with PET were correlated with thermodilution, both for the entire material and divided into groups of central and peripheral injections. Also, the values of CO from 2 different PET observers were compared. To investigate systematic errors in CO measurement, Bland–Altman plots (*6*) were used. The lung-uptake %ID, both absolute values and in relation to the first baseline scan in each animal, was correlated with indices of pulmonary pressures, CO, and LV function. $P < 0.05$ was considered significant.

RESULTS

Hemodynamic Results

Most relevant invasive measurements and calculations based on PET measurements are presented in Table 1. CO_{thermo} ranged from 2.1 to 8.2 L/min. In 1 pig we failed to obtain reliable PCWP measures. In the remaining 20 experiments, PCWP ranged from 6 to 14 mm Hg. Repeated baseline measurements were not significantly different from the first baseline in any of the studied variables.

TABLE 1
Results of Invasive Measurements and PET Measurements

Study type	No. of studies*	CO_{thermo} (L/min)	HR (min^{-1})	PCWP (mm Hg)	SV_{norm} (% of baseline)	RV-CO_{PET} (L/min)	LV-CO_{PET} (L/min)	Lung-uptake (%ID)	Normalized lung-uptake (% of baseline)
Base 1	5 (4)	4.0 ± 0.2	98 ± 7	7 ± 1	100	4.4 ± 0.5	4.2 ± 0.4	3.8 ± 0.7	100
Base 2	4 (3)	3.6 ± 0.6	95 ± 11	7 ± 1	95 ± 11	4.4 ± 0.8	3.8 ± 0.4	3.7 ± 0.7	106 ± 15
Dobut	6 (5)	6.6 ± 1.4	130 ± 11	7 ± 1	123 ± 18	6.9 ± 1.0	6.4 ± 1.3	3.6 ± 0.3	93 ± 12
Metop	6 (5)	3.0 ± 1.0	85 ± 17	9 ± 1	81 ± 13	3.2 ± 1.0	3.1 ± 0.9	5.7 ± 1.9	141 ± 34
Angioten	3	4.0 ± 0.2	105 ± 14	13 ± 1	90 ± 2	4.0 ± 0.6	3.6 ± 0.2	4.3 ± 0.7	126 ± 10

*Numbers in parentheses refer to PCWP.

CO_{thermo} = estimates of CO based on invasive thermodilution; SV_{norm} = stroke volume, normalized to baseline study in each animal; RV-CO_{PET} and LV-CO_{PET} = noninvasive CO estimates derived from PET-based analysis of first-pass activities in RV and LV ROI, respectively; Base 1 = baseline study; Base 2 = repeated baseline study; Dobut = infusion of dobutamine (20–25 μg/kg/min); Metop = combined high-dose injection of β-blocking agent metoprolol and morphine; Angioten = infusion of angiotensinamide (2.5 mg/kg/min).

Estimates of CO_{PET}

Values of CO_{PET} were highly and linearly correlated with CO_{thermo} (Figs. 2A and 3A), regardless of whether RV or LV ROIs were used for first-pass analysis.

We found a regression line of RV-CO_{PET} = 0.92 ± 0.06 × CO_{thermo} + 0.71 ± 0.26 (SEE = 0.45 L/min, r = 0.96; Fig. 2A). A Bland–Altman plot did not reveal any significant deviation from the line of unity, but a systematic and significant overestimation of CO_{PET} by a mean of 8% was seen (Fig. 2B).

When LV-CO_{PET} was used, the correlation was described by the equation LV-CO_{PET} = 0.89 ± 0.04 × CO_{thermo} + 0.5 ± 0.19 (SEE = 0.3 L/min, r = 0.98; Fig. 3A). In this case, a Bland–Altman plot revealed a small, but significant, systematic deviation from the line of unity (Fig. 3B). The relation between LV-CO_{PET} and CO_{thermo} was not significantly altered after correction for pulmonary uptake.

The AUC_{fp} values calculated from RV cavity ROIs were closely and linearly correlated with LV values (RV = 0.935 × LV; r = 0.996, $P < 0.001$). The relation between RV and LV values was equally good, regardless of the amount of injected dose.

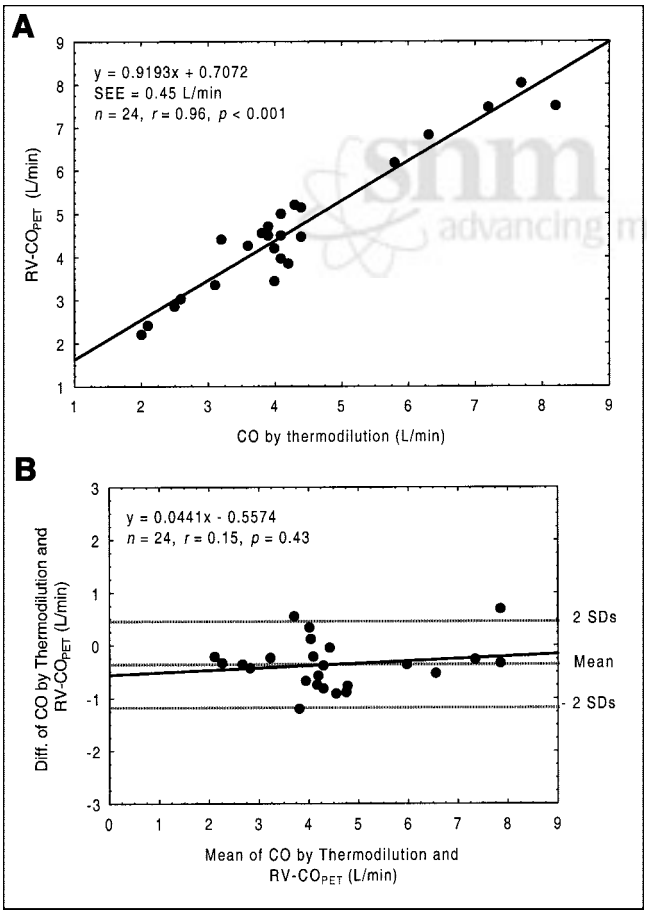

FIGURE 2. (A) Plot of estimates of CO_{PET} derived from RV ROI (RV-CO_{PET}) against standard thermodilution technique (CO_{thermo}). (B) Bland–Altman plot shows difference (Diff.) between 2 methods plotted against mean values. Slope of regression line is not significantly different from 0, but values of RV-CO_{PET} are 0.3 ± 0.4 L/min higher than CO_{thermo} ($P < 0.001$). Difference is probably due to partial-volume effects.

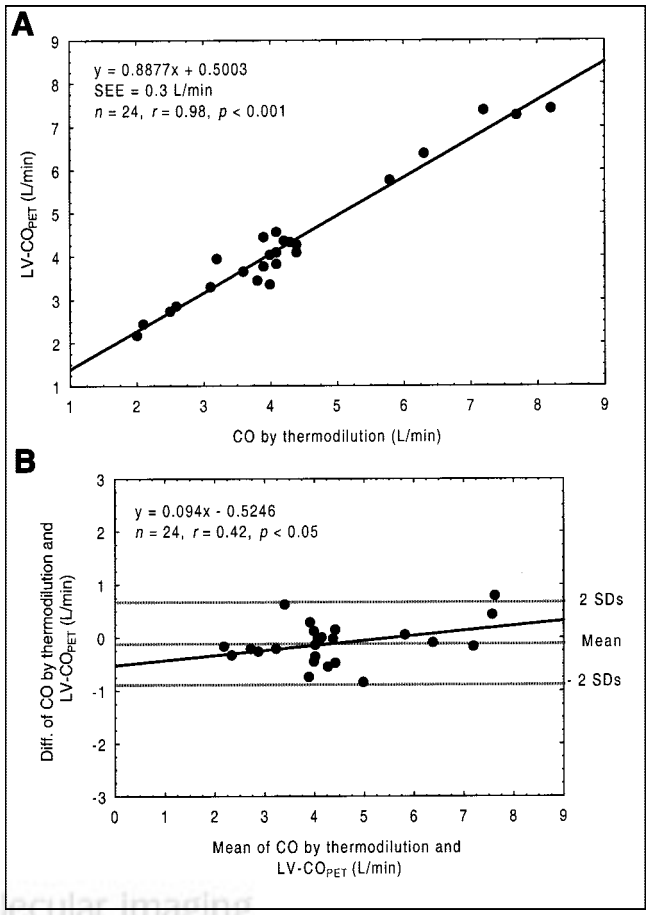

FIGURE 3. (A) Plot of estimates of CO_{PET} derived from LV ROI (LV-CO_{PET}) against standard thermodilution technique (CO_{thermo}). (B) Bland–Altman plot shows difference (Diff.) between 2 methods plotted against mean values. Slope is significantly different from 0.

When the peripheral vein was used for tracer injection, bolus fractionation was seen in 5 of 10 cases and resulted in a variable downward slope of the first-pass curve. This was slightly more prominent in the LV, in which distinguishing between the tail of the first pass and the recirculation was difficult in 2 of 10 cases (studies 2 and 3 in pig 5). RV-CO_{PET} and LV-CO_{PET} values from the 10 peripheral vein experiments plotted separately against CO_{thermo} resulted in slopes of 0.98 and 0.88, respectively.

Interobserver correlation of LV-CO_{PET} estimates by observers 1 and 2 was r = 0.98 (Fig. 4). The mean variability between observations was 6%. A similar evaluation of RV-CO_{PET} revealed r = 0.92, $P < 0.001$.

The myocardial net extraction rate of acetate (K1) was highly and linearly correlated with RPP (K1 = 0.00004 × RPP + 0.08; n = 24, r = 0.94, $P < 0.001$). The difference between CO_{thermo} and LV-CO_{PET} (corrected for pulmonary uptake) showed a positive and near-significant relation to

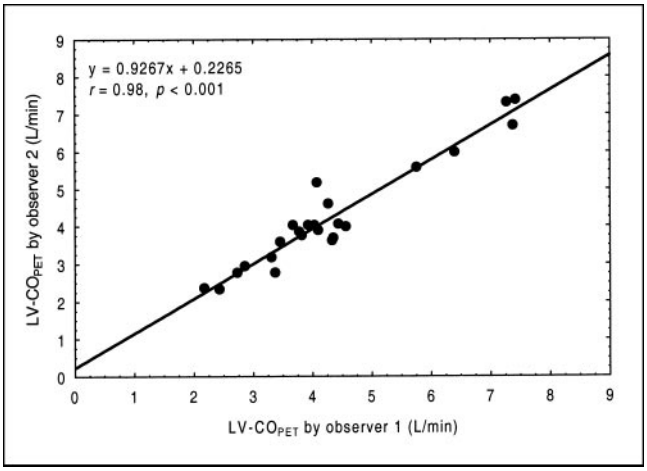

FIGURE 4. Plot of estimates of CO_{PET} derived from LV ROI (LV-CO_{PET}) by 2 observers. Observer 2 performed all postprocessing steps but was unaware of all other data. Correlation between estimates was highly significant ($r = 0.98$, $P < 0.001$), indicating that PET method is well reproduced. Interobserver variability was calculated to be 6%.

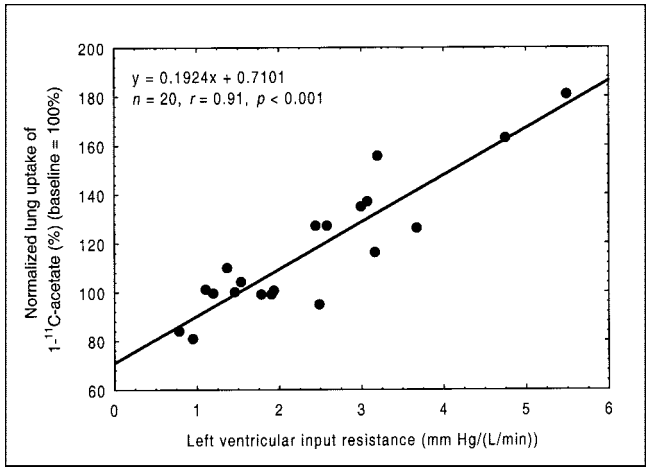

FIGURE 5. Plot of pulmonary uptake of 1-^{11}C-acetate, normalized to baseline values, in relation to invasively derived LV input resistance, calculated as PCWP divided by CO. Linear and highly significant correlation was found ($r = 0.91$, $P < 0.001$), suggesting that alterations in pulmonary tracer uptake are primarily affected by capillary transit time and left atrial pressure.

myocardial uptake rates ($r = 0.39$, $P = 0.06$). No such trend was found when RV-CO_{PET} was similarly evaluated.

Pulmonary Uptake of 1-^{11}C-Acetate and Relation to Flow and Pressures

Pulmonary extravascular retention of ^{11}C was constant from 2 to 4 min after injection The lung-uptake %ID was 4.3 ± 1.3 %ID (range, 2.7–8.5 %ID). Relatively large variations were found, both between different animals and between serial studies. An obvious uptake gradient in the direction of gravity was seen in all studies. Signs of progressive atelectasis formation, localized dorsally in the direction of gravity, were found in all pigs at serial scan comparison. This was noted as an increasing regional absence of air on transmission scans, blood-pool increases, and relatively extreme localized acetate retention.

Total lung volumes ranged from 670 to 960 mL. Only minor changes in lung volumes were detected in serial measurements. The blood fraction, measured by ^{15}O-CXO (2 experiments in each of 3 animals), of total lung volume was 17.3% ± 1.2%. The estimated activity of ^{11}C in lung blood from 2 to 4 min after injection was 12.3% ± 3.3% of the total lung ^{11}C activity.

The lung-uptake %ID was inversely correlated with CO ($n = 24$, $r = -0.63$, $P = 0.006$) and positively correlated with LV input resistance ($n = 20$, $r = 0.79$, $P < 0.001$), but it was only weakly related directly to PCWP ($n = 20$, $r = 0.40$, $P = 0.08$). The lung-uptake %ID, normalized to baseline, correlated linearly with LV input resistance ($n = 20$, $r = 0.91$; Fig. 5) and curvilinearly with PCWP ($n = 20$, $r = 0.56$, $P = 0.01$; not shown). No significant relation was found between lung-uptake %ID and RVascPulm or PA pressures.

A strong correlation was also found when comparing normalized lung-uptake %ID to normalized SV ($n = 24$; linear correlation: $r = -0.77$, $P < 0.001$; Fig. 6). As evident in the diagram in Figure 6, the relation is nonlinear and changes in lung-uptake %ID were more pronounced when SV decreased. Fitting a piecewise linear regression with a breakpoint set to baseline (i.e., 100%) increased the r value to 0.90. Automated software best-breakpoint generation increased the r value to 0.95 at a breakpoint of 112%, which was significantly better than the correlation coefficient established by the simple linear regression analysis ($P < 0.005$).

DISCUSSION

The primary aim of this study was to investigate the feasibility of a very simple method of analysis in determin-

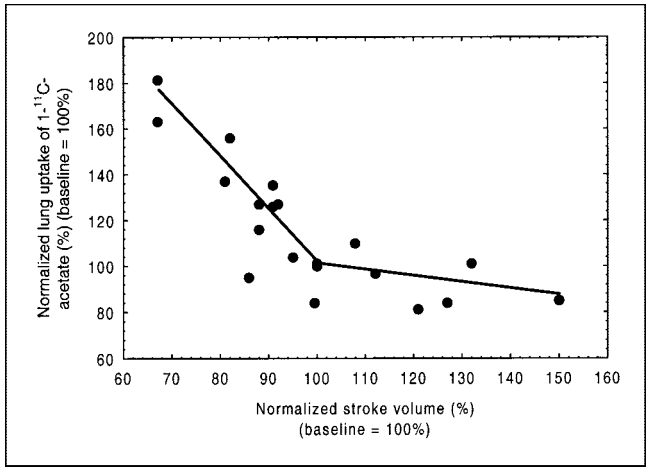

FIGURE 6. Plot of pulmonary uptake of 1-^{11}C-acetate in relation to SV. Both variables were normalized to values obtained at initial baseline scan in each animal. Plot shows that marked elevation of pulmonary tracer uptake occurs when LV contractility is lowered. This relation was best fitted by piecewise linear regression algorithm ($r = 0.95$, $P < 0.001$).

ing CO by the indicator dilution principle using standard PET techniques and simple calculations in commercially available software. The method was found to be accurate and reproducible.

Traditionally, when CO is determined by rapid sampling of concentrations of dye or radioactivity in arterial blood, fitting a gamma-variate function to the time–activity curve separates the first pass and the recirculation. This approach requires a rapid bolus without fractionation, more important when a nonextractable dye or tracer is used. If peripheral extraction is 100%, as for microspheres, there will be virtually no recirculation. Because some clinically used PET scanners, like the one we used, only give reliable values for time frames of 5 s or more, the first pass through the LV might be contained in as few as 2 or 3 time frames. So few time points are not suitable for curve-fitting purposes. However, some partially extracted tracers such as ^{11}C-acetate have a high systemic first-pass extraction and very little indicator is recirculated, thereby mimicking microspheres. This introduces a situation in which activity is zero in the frame before bolus arrival and again near zero in a short time frame after the bolus transit is complete. In this situation, curve fitting and rapid sampling are not needed to calculate the AUC_{fp} because the sum of products of each individual time frame (min) and the corresponding mean activity (Bq/mL) would constitute the actual AUC_{fp}.

To our knowledge, the application of CO measurements by the indicator dilution principle with PET has only been reported once earlier. In a study by Chen et al. (*7*), PET was compared with a previously validated gamma-camera–based method in 14 patients. The PET tracer used was ^{82}Rb, which is another partially extractable tracer of myocardial flow, and the calculation of CO was done by fitting a gamma-variate curve to a time–activity curve derived from an LV ROI. The authors found a good agreement between methods, but no error analysis was used. There was a slight underestimation of CO_{PET} at higher flows, but this was not commented on.

In this study, we also found a slight underestimation of LV-CO_{PET} in high output situations. Because myocardial tissue uptake of both ^{82}Rb and 1-^{11}C-acetate are flow dependent, increasing spillover from the myocardial wall into the LV cavity ROI would be expected when MBF is elevated. This increased spillover would then increase the LV-AUC_{fp}, which again would decrease the resulting CO estimate. Although not truly statistically significant, a relation between CO underestimation and MBF was found in this study.

Because errors in CO calculated from RV did not show any relation to MBF, this would favor the use of RV as the region of choice. On the other hand, RV-CO_{PET} was slightly higher than both LV-CO_{PET} and CO_{thermo} in most cases. A probable explanation of this finding is the problem of the partial-volume effect, meaning that PET underestimates regional activity when small structures are studied. This problem has been studied in depth in relation to myocardial PET (*8*) and to some extent depends on hardware issues such as filtering and scanner resolution, but will also occur when a static ROI is placed on a moving object such as the heart. Earlier phantom studies (*5*), using the same scanner as that used in this study, imply that activity recovery from spheric objects decreases linearly from 100% at a diameter of 35 mm to 80% at a diameter of 17 mm. The RV in pigs is narrower than in humans and the observed mean error of 8% underestimation of the AUC_{fp} would probably be smaller or absent in most adult human studies.

In this study, HRs were in some cases found to vary extensively during a single PET study, suggesting that we were not able to maintain perfect steady-state conditions in all cases. We averaged the HR over the time it took to perform the thermodilution measurements and, even without evidence of arrhythmia, HRs varied by up to 20% in some cases. This problem might explain some of the deviations from unity detected in our comparisons.

Delimiting the first pass from the recirculation was done interactively by a simple cutoff, posing a problem if recirculation occurs very early in combination with extensive tracer dispersion. Due to the high systemic first-pass extraction of acetate, only small amounts of recirculated activity were seen in the experiments and defining the end of the first pass was straightforward. This might not be the case if a tracer with a lower systemic extraction fraction—for example, ^{18}F-FDG—is used. In that case, the RV approach is preferable and the bolus administration should be more rigorously controlled.

When CO is measured by the indicator dilution principle and the use of curve-fitting procedures, bolus fractionating is not well tolerated. Still, in clinical practice irregular boluses occur frequently and introduce some subjectivity in curve positioning. According to the stimulus–response theorem (*9*), fractionation is not a problem per se, as long as data can be corrected for recirculation. Irregular boluses were admitted when the peripheral vein was used and measurements were equally as stable as when the bolus was injected directly in the superior vena cava. Accordingly, this observation suggests the proposed method is stable in terms of different injection techniques.

Correcting the injected dose for pulmonary loss of activity did not alter the slope of the relation of LV-CO_{PET} toward CO_{thermo} and moved the *y*-intercept insignificantly toward zero. Statistically, this is of course a matter of sample size. We found the average early lung uptake of labeled acetate in pigs to be approximately 4% of the injected dose. In the most extreme case, a deposition of 8% was found. Whether these figures apply to humans is not known, but even higher uptake should be expected in advanced pulmonary congestion. For this, and the other reasons mentioned above, we recommend the use of the RV approach in the clinical situation.

Although the fate of extracted acetate in lung tissue is not known, the observations in this study indicate that pulmonary transcapillary fluxes of acetate appear to be primarily

passive processes. A little surprising, the pulmonary uptake of labeled acetate was inversely correlated with CO. As total pulmonary blood flow equals CO, this finding suggests a strong positive relation between capillary transit time and acetate transudation rate.

Only small variations in PCWP were found. Although relative increases of 70%–100% in PCWP were induced in 3 of 4 pigs, absolute values only varied between 6 and 14 mm Hg. Still, we found a positive relation of lung uptake to PCWPs, indicating that lung uptake is positively affected by LV filling pressures.

Combining PCWP and CO into an index of LV input resistance is of course nonstandard but, nonetheless, seems to describe well the determinants causing the observed changes in pulmonary acetate uptake.

As CO and PCWP were altered primarily by inotropic stimulation and inhibition and, thereby, induced significant changes in myocardial contractility, there is also an indication that LV function is a major determinant of pulmonary transudation rates. In our study, this is reflected in the finding of a strong negative and piecewise linear relation between relative SVs and relative pulmonary uptake of tracer, a relation that by itself explains almost all of the observed variation ($R^2 = 0.92$). This is in line with a common observation in clinical nuclear cardiology studies, performed with ^{201}Tl, in which an elevated lung/heart uptake ratio after stress indicates a left heart backward failure and supports the diagnosis of ischemia-induced LV insufficiency (*10,11*). More studies are needed to define the usefulness of the current observations.

In the foreseeable future, there is probably no place in routine clinical practice for a PET method with the only goal of measuring CO, however accurate. The usefulness of this technique, and the reason why we undertook this study, would become apparent when there is a need to assess hemodynamic indices in relation to the already established uses of myocardial PET. The commonly used myocardial PET tracers, such as ^{13}N-ammonia and ^{18}F-FDG, might gain incremental clinical value by incorporating this concept. Especially the evolving use of electrocardiographically gated FDG PET for calculation of LV ejection fraction and total SV (*12*) might gain synergistic effects by implementing forward SV assessment, because this makes estimates of regurgitant volumes possible.

Our data provide some validation of the use of a RV ROI as input function, which opens up new interesting possibilities. For example, because virtually no indicator is lost from the site of injection in a peripheral vein to the RV, any injectable positron-emitting tracer functions in the assessment of CO.

We chose to test the feasibility of hemodynamic measurements by PET with 1-^{11}C acetate for a number of reasons. Apart from the obvious benefits of having access to accurate and simultaneous data on both MBF and oxidative metabolism in a single noninvasive investigation, the addition of equally accurate and simultaneous hemodynamic data of heart pump function and pulmonary adaptations expands the utility of the investigation greatly. As already proposed, a WMI can be constructed by multiplying 3 indices of myocardial work (i.e., SV index, HR, and systolic blood pressure) and dividing the resulting product with an index of the myocardial oxidative metabolic rate derived from the AC-PET study. The WMI thereby mirrors the metabolic cost of the LV mechanical work. In recent studies using this concept, SV was assessed by MRI, radionuclide ventriculography, or 2-dimensional echocardiography (*3,13,14*). These approaches have proven to be feasible and the authors were able to detect significant changes in small patient groups. However, measuring SV directly from the dynamic PET data might have lowered the study costs. Because of the simultaneous acquisition of all parameters, it might also have increased the accuracy of the WMI calculations.

One of the main limitations of this study is the small number of animals. We suggest, however, that the total number of experiments suffice in validating CO measurements by PET using this simple protocol. We also managed to induce sufficient spread in CO data to allow some conclusions about the impact of possible error sources to be drawn.

Direct measurement of left heart pressures would have improved the validity of our conclusions regarding the pulmonary uptake of acetate. In our experience, pigs are quite vulnerable to invasive left heart manipulations and we might not have been able to keep the animals alive through extensive serial studies. Given the results of our study, a more elaborate experimental protocol could be well rewarded.

CONCLUSION

We have shown that the noninvasive measurement of CO_{PET} is feasible over a wide range of COs. Potential error sources appear to be within acceptable limits. The method is easily taught, and work-up is simple and adds a minor overhead to the postprocessing time. The technique is directly applicable in most PET facilities without any special added requirements and appears to be easily incorporated into existing dynamic myocardial PET protocols with no extra costs. This might increase the clinical utility of most cardiac PET studies. We also reported on the possibility of noninvasively estimating left atrial filling pressures indirectly by PET by quantifying first-pass tracer uptake in lung tissue. Further evaluation of the significance of the pulmonary retention of labeled acetate in humans is needed and might prove valuable.

REFERENCES

1. Klein LJ, Visser FC, Knaapen P, et al. Carbon-11 acetate as a tracer of myocardial oxygen consumption. *Eur J Nucl Med.* 2001;28:651–668.
2. van den Hoff J, Burchert W, Borner AR, et al. 1-^{11}C-Acetate as a quantitative perfusion tracer in myocardial PET. *J Nucl Med.* 2001;42:1174–1182.
3. Bengel FM, Permanetter B, Ungerer M, Nekolla S, Schwaiger M. Non-invasive estimation of myocardial efficiency using positron emission tomography and

carbon-11 acetate: comparison between the normal and failing human heart. *Eur J Nucl Med.* 2000;27:319–326.
4. Weisel RD, Berger RL, Hechtman HB. Measurement of cardiac output by thermodilution. *N Engl J Med.* 1975;292:682–684.
5. Adam L, Zaers J, Ostertag H, Trojan H, Bellemann ME, Brix G. Performance evaluation of the whole-body PET scanner ECAT EXACT HR+ following the IEC standard. *IEEE Trans Nucl Med.* 1997;44:1172–1180.
6. Bland JM, Altman DG. Statistical methods for assessing agreement between two methods of clinical measurement. *Lancet.* 1986;1:307–310.
7. Chen EQ, MacIntyre WJ, Fouad FM, et al. Measurement of cardiac output with first-pass determination during rubidium-82 PET myocardial perfusion imaging. *Eur J Nucl Med.* 1996;23:993–996.
8. Boyd HL, Gunn RN, Marinho NVS, et al. Non-invasive measurement of left ventricular volumes and function by gated positron emission tomography. *Eur J Nucl Med.* 1996;23:1594–1602.
9. Lassen NA, Perl W. *Tracer Kinetic Methods in Medical Physiology.* New York, NY: Raven Press; 1979:38–49.
10. Mannting F. Pulmonary thallium uptake: correlation with systolic and diastolic left ventricular function at rest and during exercise. *Am Heart J.* 1991;119:1137–1146.
11. Marcassa C, Galli M, Baroffio C, Eleuteri E, Campini R, Gianuzzi B. Independent and incremental prognostic value of ^{201}Tl lung uptake in patients with severe postischemic left ventricular dysfunction. *Circulation.* 2000;102:1795–1801.
12. Hattori N, Bengel FM, Mehilli J, et al. Global and regional functional measurements with gated FDG PET in comparison with left ventriculography. *Eur J Nucl Med.* 2001;28:221–229.
13. Bengel FM, Nekolla SG, Ibrahim T, Weniger C, Ziegler SI, Schwaiger M. Effect of thyroid hormones on cardiac function, geometry, and oxidative metabolism assessed noninvasively by positron emission tomography and magnetic resonance imaging. *J Clin Endocrinol Metab.* 2000;85:1822–1827.
14. Beanlands RS, Nahmias C, Gordon E, et al. The effects of $beta_1$-blockade on oxidative metabolism and the metabolic cost of ventricular work in patients with left ventricular dysfunction: a double-blind, placebo-controlled, positron-emission tomography study. *Circulation.* 2000;102:2070–2075.